Vibrational Spectra, Orientations, and Phase Transitions in Long-Chain Amphiphiles at the Air/Water Interface: Probing the Head and Tail Groups by Sum Frequency Generation

D. Zhang, J. Gutow, and K. B. Eisenthal*

Chemistry Department, Columbia University, New York, New York 10027

Received: September 13, 1994[⊗]

IR + visible sum frequency generation (SFG) has been used to obtain the vibrational spectra and orientations for both the nitrile (CN) head group and the methyl (CD_3) tail of the insoluble long-chain amphiphile $CD_3(CH_2)_{19}CN$ at the air/water interface. The results show that the orientations of the head group and the terminal group vary with amphiphile surface density, but in markedly different ways. It is found at the amphiphile density, which corresponds to the phase transition from the gas/liquid coexistence region to the liquid region, that the hydrogen bonds of the CN head groups to water are broken, the water is squeezed out of the monolayer, and the orientation of the head group changes sharply. The possibility that the rupturing of the hydrogen bonds and reorientation of the CN head groups may be the trigger for the phase transition is discussed. In addition to the SFG study of the amphiphile at the air/water interface, a method was discovered that enables SFG to remove the ambiguity in the ratio of the two Raman polarizability elements for a symmetric stretch. Depolarization measurements in linear Raman experiments cannot determine whether the ratio of elements is greater than or less than one, whereas the SFG method can.

Introduction

The special chemical and physical properties of insoluble long-chain amphiphiles at aqueous interfaces, often referred to as Langmuir monolayers, have long fascinated scientists and been the subject of intense study. The organization of these amphiphiles into myriad structures and phases is responsible for the enormous range and variation in their properties. The various structures are dependent on the interactions of the hydrocarbon chains and the hydrophilic head groups within the monolayer as well as their interactions, primarily the head group, with the aqueous subphase. In recent years the application of X-ray diffraction,[1] neutron scattering,[2] reflection IR spectroscopy,[3] fluorescence,[4,5] and the nonlinear spectroscopies such as second harmonic generation (SHG)[6] and IR + visible sum frequency generation (SFG)[7,8] have made it possible to investigate these monolayers at the molecular level.

From these various studies, the general view has emerged that the hydrophilic head group maintains a relatively constant orientation at the liquid interface as the density of the monolayer varies, while the hydrophobic tail lies down on the surface in a random coil at low density and becomes more upright and constrained as the monolayer is compressed.[9,10] A pioneering SFG study[11] in the C−H vibrational region of pentadecanoic acid ($CH_3(CH_2)_{13}COOH$) spread on water yielded results consistent with this description of the hydrocarbon chain orientation at low and high densities. The orientation of the head group, however, as a function of density has not been explored to our knowledge. The work reported here demonstrates for the first time how the interface and chromophore selectivity of SFG can be used to get spectroscopic and structural information on both ends of an amphiphile, thereby providing a more complete physical picture of the behavior of Langmuir monolayers.

Our results on the CD_3 and CN groups of the terminally deuterated long-chain cyanide (1-cyanoeicosane, $CD_3(CH_2)_{19}CN$) at an air/water interface show that the orientations of both the head group and the terminal methyl group change with surface density but have different density dependencies. Of marked interest are the results that the hydrogen bonds of water to the CN head group are broken when the monolayer is compressed to a density just past the coexistence to liquid phase transition density, i.e., into the liquid regime of the amphiphile phase diagram. This observation suggests that a key step in the phase transition requires the water molecules located between the nitrile head groups to be squeezed out of the liquid phase monolayer.

Experimental Methods

The sum frequency experiments were performed by focusing the visible and infrared radiation to a common spot on the surface of interest in a counter propagating geometry at an angle of 70° from the surface normal, as shown in Figure 1. The visible beam used for the SFG experiments is a small portion (~150 μJ/pulse) of the 532-nm output from a Continuum YAG-501C (~20 ps pulses at 10 Hz). The infrared radiation is generated by difference-frequency mixing in a 20-mm $LiIO_3$ crystal, using approximately 1.5 mJ/pulse of the YAG green and the ~1 mJ/pulse tunable output from a dye laser (Continuum PTL10, pumped by 80% of the YAG green output, generating ~15-ps pulses). The apparatus can produce 40−50 μJ/pulse IR between 1900 and 2600 cm^{-1}. The IR radiation has a bandwidth of 7−10 cm^{-1} FWHM, a pulse duration approximately the same as that of the dye laser (~15 ps), and its frequency was calibrated to ±1.5 cm^{-1} with use of the deuterated acetonitrile absorption spectrum.

Except as noted in the text, both incoming beams are polarized at 45° to the surface normal and parallel to each other. The sum frequency signal is collected at approximately 50° from the normal to the surface as dictated by the wave vector matching conditions.[12] The signal is separated from the background by using a combination of apertures, interference filters, and a monochromator. A sheet polarizer is used to analyze the polarization of the signal and an achromatic-halfwave plate (Special Optics) is used to rotate the polarization of the SF signal to the orientation that is most efficiently

* To whom correspondence should be addressed.
[⊗] Abstract published in *Advance ACS Abstracts,* December 1, 1994.

0022-3654/94/2098-13729$04.50/0

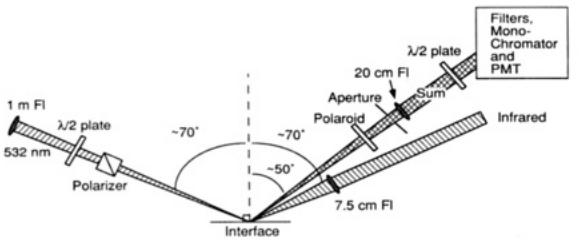

Figure 1. Schematic of surface sum frequency experimental apparatus.

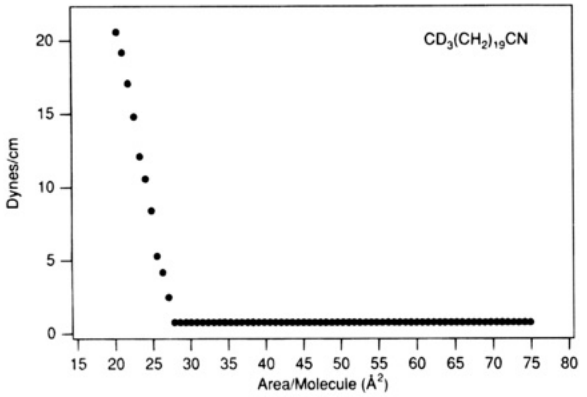

Figure 2. Pressure−area (Π−*A*) isotherm for $CD_3(CH_2)_{19}CN$ spread at the air/water interface.

transmitted by the monochromator (see Figure 1). For the data presented here, each point is the average signal from 3000 laser shots. The resonant signal levels correspond to a photon every few laser shots.

The surface pressure (Π) versus surface area (*A*, area/molecule) isotherm of $CD_3(CH_2)_{19}CN$ spread on water was measured by using a Langmuir trough and Wilhelmy balance at 25 °C.[9] The isotherm is shown in Figure 2. The samples for the SFG experiments were prepared by spreading the long-chain cyanide onto double-distilled water in Teflon containers from a 10^{-4} M solution in hexane (HPLC, Aldrich). Evaporation of the water subphase was prevented by placing the sample container in a sealed glass and Teflon housing during the experiment.

The deuterated long-chain cyanide ($CD_3(CH_2)_{19}CN$) was synthesized from $CD_3(CH_2)_{19}Br$ (98 atom % D, Cambridge Isotope Labs) by nucleophilic substitution using NaCN (Aldrich) in *N*,*N*-dimethylacetamide (99+%, Janssen Chimica). The desired compound was extracted with hexane (HPLC, Aldrich) and recrystallized from a 2:1 ethanol:water solution. Purity was found to be better than 98% by NMR and GC.

Results and Discussion

Figure 2 shows the pressure−area (Π−*A*) isotherm for the $CD_3(CH_2)_{19}CN$ spread on water. These results are similar to those of Copland and Harkins for octadecane nitrile ($CH_3(CH_2)_{16}CN$).[13] The flat region in the isotherm at an area greater than 27 Å^2/molecule is the gas−liquid coexistence region. In this density region the interface is inhomogeneous and consists of condensed islands coexisting with isolated molecules.[9] The amphiphile density within the condensed islands is 27 Å^2/molecule, which is the liquid phase density at the phase transition point that connects the coexistence and liquid phases. Second-harmonic generation studies of the fluctuation in the nonlinear signal associated with the translational motion of these islands for other amphiphiles have been reported.[14] These studies found that most of the signal comes from the condensed islands. At the densities used in the studies reported here the

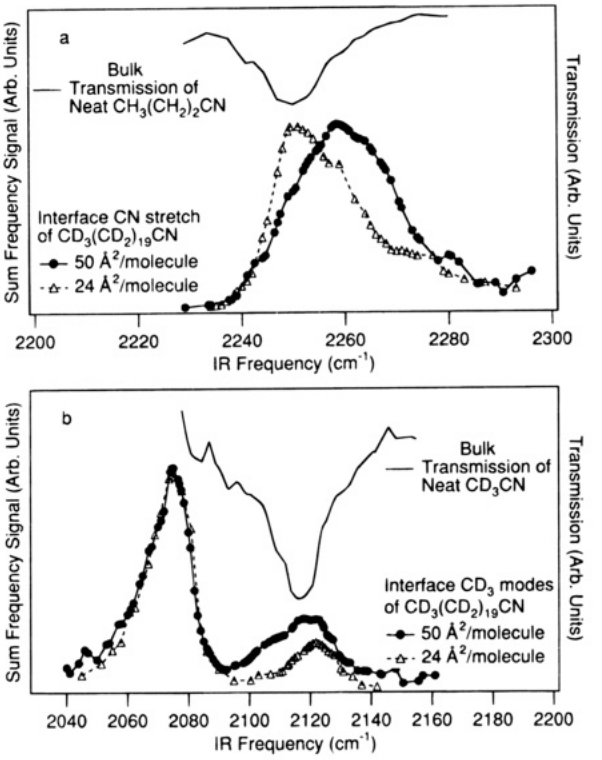

Figure 3. (a) Upper trace is a transmission spectrum of a neat bulk $CH_3CH_2CH_2CN$ sample. The two bottom traces are sum frequency spectra of the CN vibration of $CD_3(CH_2)_{19}CN$ at 24 and 50 Å^2/molecule. (b) The upper trace is a transmission spectrum of a neat CD_3CN sample. The two bottom traces are sum frequency spectra of the CD_3 modes of $CD_3(CH_2)_{19}CN$ at 24 and 50 Å^2/molecule. The more intense band is the symmetric stretch and the weaker one is a Fermi resonance overtone of the methyl deformation with the symmetric stretch.

sum frequency signal in the coexistence region is similarly dominated by the condensed islands and not the very low density gas region of the surface. The SFG signal should therefore be characteristic of the liquid state of the monolayer at the transition point of 27 Å^2/molecule. The regions below 27 Å^2/molecule are the higher density liquid and solid regions. Our sum frequency experiments were performed on samples spread at between 100 and 22 Å^2/molecule, which extends from the gas−liquid coexistence region into the liquid-phase region.

Figure 3 shows sum frequency spectra of the CN and CD_3 regions of the long-chain nitrile at 24 Å^2/molecule, which is in the liquid phase region, and 50 Å^2/molecule, which is in the gas−liquid coexistence region. The CN sum frequency spectra look very different at these two densities, as shown in panel a. At the density of 24 Å^2/molecule, we observed an absorption peak at the frequency of the bulk CN vibration. At the lower surface density, 50 Å^2/molecule, the peak is shifted to higher energy and exhibits a larger bandwidth than in the liquid-phase region. The FWHM of the sum frequency peak at low density is ~24 cm^{-1} and at high density it is ~18 cm^{-1}. The frequency shift of the CN vibration is similar to the shift we have previously reported for acetonitrile at the air/acetonitrile−water solution interface.[15] As with acetonitrile we attribute the blue shift in the frequency of the CN vibration relative to that of the neat bulk CN vibration to the hydrogen bonding of the nitrile head groups with water molecules in the gas−liquid coexistence region. When the monolayer is compressed into the liquid-phase region, the water molecules between the head groups are squeezed out of the monolayer, which involves breaking the hydrogen bonds, and this results in a shift of the CN vibration of the liquid-phase monolayer back to the CN bulk value.

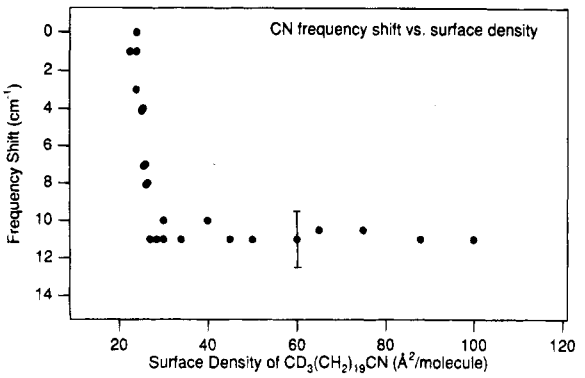

Figure 4. Compilation of frequency shifts of the CN resonance peak versus area per molecule of $CD_3(CH_2)_{19}CN$ at the air/water interface.

In order to obtain a more complete physical picture of the behavior of the CN head group of $CD_3(CH_2)_{19}CN$, we have examined the orientation and vibrational frequency of the CN group versus amphiphile surface density. Figure 4 shows the frequency shift for the CN stretching vibration as a function of surface density. It is seen that the CN frequency is blue-shifted by ~10 cm^{-1} throughout the gas−liquid coexistence region. This suggests that the chemical environment around the nitrile head group is the same throughout the gas−liquid coexistence region. At these densities, manifested by the blue shift in the CN vibration, the head groups are hydrogen bonded and solvated by water molecules. As the density increases very slightly beyond the phase transition point of 27 $Å^2$, there is a sharp red shift in the CN vibrational frequency, reaching a frequency equal to that of the CN neat bulk value. The red shift in the vicinity of the phase transition indicates that the water molecules solvating and hydrogen bonded to the nitrile head groups are squeezed out of the monolayer, breaking the hydrogen bonds and generating the observed shift. It should be noted that at 27 $Å^2$/molecule, which is the amphiphile density of the condensed islands throughout the coexistence region, the CN groups are still hydrogen bonded and thus their frequencies are blue-shifted with respect to that of neat bulk CN.

The more intense transition in the methyl group spectrum (Figure 3b) is the methyl symmetric stretch and the weaker transition, assigned to the first overtone of the methyl deformation,[16,17] arises from Fermi resonance with the symmetric stretch. Just as with the methyl vibration of deuterated acetonitrile[15] the symmetric stretching frequency of the methyl group of the long-chain nitrile is insensitive to the density of molecules in the interface. However, for the overtone, we observed about a 5-cm^{-1} shift to higher energy from 2119 cm^{-1} in the gas−liquid coexistence region up to 2124 cm^{-1} in the liquid phase, which is consistent with the fact that overtones are often more sensitive to the local environment. Studies of alkane overtones have shown that increased crowding, both inter- and intramolecular, of the CH oscillators tends to decrease the anharmonicity of the C−H potential and thus increases the frequency at which the overtones are observed.[18,19] As with the CN vibration, the overtone bandwidth increases from ~15 cm^{-1} for the liquid phase to ~25 cm^{-1} for the gas−liquid coexistence region. This increase in bandwidth is believed to reflect a larger variety of local environments for the tail in the coexistence region than in the more compressed liquid-phase region.

We now consider results on the polarization of the sum frequency signal, which provides information on the orientations of the head and tail groups of the amphiphile. The variation in the polarization of the sum frequency signal with surface density, when both input beams are polarized at 45° to the surface normal, is shown in Figure 5. It is seen that the polarization of

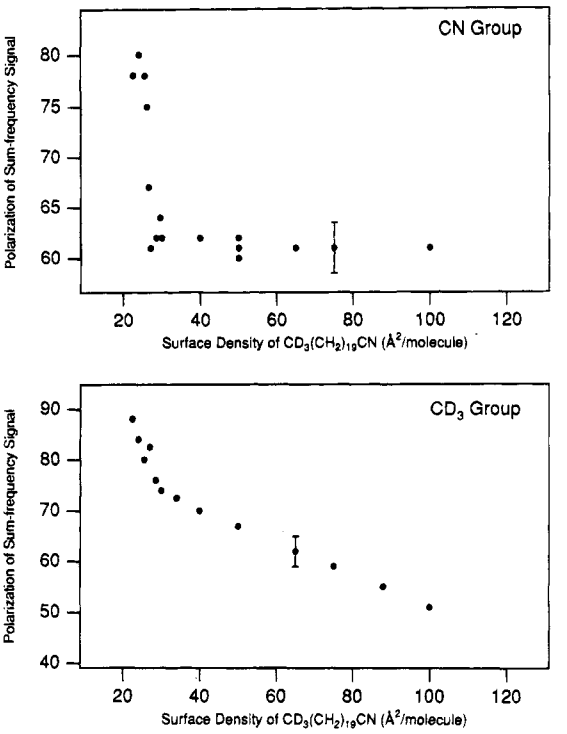

Figure 5. Compilation of the polarization of the resonant sum frequency signal versus monolayer density for the CN head group and the CD_3 tail.

the SFG signal from the CN (head group) remains constant throughout the gas−liquid coexistence region, but becomes more s-polarized, i.e., polarized parallel to the surface, after the monolayer is compressed into the liquid phase. The polarization of the signal from the symmetric stretch of the terminal methyl group, however, behaves differently. The signal becomes more s-polarized as the monolayer density increases even in the coexistence region. Nonetheless, the transition to the homogeneous liquid phase at the 27 $Å^2$/molecule transition density is still observable as a change in slope of the CD_3 polarization versus density. These results show that the average orientations of the two ends of the amphiphile depend differently on the density. For the CN head group, its average orientation is constant as the density varies in the coexistence region, due to the fact that the intermolecular separation between CN head groups in the liquid density islands remains the same as at 27 $Å^2$/molecule throughout the coexistence region. The orientation of the CN changes when the transition from the coexistence region to the liquid region occurs, which corresponds to the molecules being squeezed to a density greater than 27 $Å^2$/molecule. We conclude from the polarization and spectral results that the reorientation occurs in parallel with the apparent rupturing of the head group hydrogen bonds to water, as seen in the CN vibrational frequency shift, which also occurs at 27 $Å^2$ (Figure 4). On the other hand our results indicate that the averaged orientational distribution for the terminal methyl group changes throughout the coexistence region. We suggest that the polarization change in the coexistence region could reflect the varying ratio of the number of molecules close to the perimeter of the liquid islands in the coexistence region. Molecules close to the perimeter can have their tails extended not only in the limited upright orientations accessible to molecules in the center of the islands but in more horizontal orientations as well. This increase in the number of possible configurations for the perimeter amphiphiles lowers the Gibbs energy and is thus favored. As we compress the monolayer and increase the surface density in the coexistence region, the

relative number of molecules close to the perimeter of the liquid- and gas-phase regions decreases, thus changing the average orientational distribution of the tails. The lack of change for the CN head groups through the coexistence region, unlike the CD_3, indicates that the orientation of CN is determined by interactions with the H_2O subphase through hydrogen bonding and solvation for both the perimeter and the interior molecules.

To estimate the orientations of the head group (CN) and the tail (CD_3) of the long-chain amphiphile, the ratio of two nonlinear susceptibility elements $\chi^{(2)}_{xxz}$ and $\chi^{(2)}_{xzx}$ was measured for each of the chromophores. The relation between the resonant surface nonlinear susceptibility $\chi^{(2)}_{ijk}$ and the nonlinear molecular polarizability $\alpha^{(2)}$, is given by

$$\chi^{(2)}_{ijk} = N \sum_{l,m,n} \langle (\mathbf{i}\cdot\mathbf{l})(\mathbf{j}\cdot\mathbf{m})(\mathbf{k}\cdot\mathbf{n}) \rangle \alpha^{(2)}_{lmn} \quad (1)$$

where N is the surface density of the molecules and the bracketed term is the ensemble average of the orientational transformation operator between the molecular and laboratory frames. From the symmetry of CN and CD_3 symmetric stretching vibrations, two molecular hyperpolarizabilities are considered here, namely, $\alpha^{(2)}_{zzz}$ and $\alpha^{(2)}_{xxz} = \alpha^{(2)}_{yyz}$, where the z axis is the three-fold symmetry axis of CD_3. If we define the molecular hyperpolarizability ratio R to be $\alpha^{(2)}_{xxz}/\alpha^{(2)}_{zzz}$ and θ to be the angle between the molecular symmetry axis and the surface normal, we then obtain

$$\chi^{(2)}_{xzx} = N(\langle \sin^2\theta \cos\theta \rangle (1 - R)/2)\alpha^{(2)}_{zzz} \quad (2)$$

$$\chi^{(2)}_{xxz} = N(\langle \cos^3\theta \rangle R + \langle \sin^2\theta \cos\theta \rangle (1 + R)/2)\alpha^{(2)}_{zzz} \quad (3)$$

In our SFG experiments, these two nonlinear susceptibilities were measured independently by using different polarization combinations, $\chi^{(2)}_{xxz}$ with ssp- (SFG, visible, and IR) polarizations and $\chi^{(2)}_{xzx}$ with sps- (SFG, visible and IR) polarizations, where p refers to the polarization in the plane of incidence (yz), while s, which is the x axis, is the component perpendicular to that plane. The surface plane is the xy plane.

Combining eqs 2 and 3 and assuming a narrow distribution of the angle θ, we can solve for θ:

$$\theta = \operatorname{arccot}\left[\left(\frac{\chi^{(2)}_{xxz}}{\chi^{(2)}_{xzx}} - \frac{1+R}{1-R}\right)\frac{1-R}{2R}\right]^{1/2} \quad (4)$$

The ratio R can be estimated from Raman depolarization ratios. Since $\alpha^{(2)}_{lmn} \propto (\alpha^{\text{Raman}}_{lm})\mu_n$, where μ_n is the vibrational transition dipole along axis n and $\alpha^{\text{Raman}}_{lm}$ is an element of the Raman polarizability tensor, then $R = \alpha^{(2)}_{xxz}/\alpha^{(2)}_{zzz} = \alpha^{\text{Raman}}_{xx}/\alpha^{\text{Raman}}_{zz}$.[20] When the transition is totally symmetric, the expression for R in terms of the Raman depolarization ratio is

$$R = \frac{Q-1}{Q+2} \text{ or } \frac{Q+1}{Q-2}, \quad Q = \left[\frac{3}{5}\left(\frac{1}{\varrho} - \frac{4}{3}\right)\right]^{1/2} \quad (5)$$

where ϱ is the Raman depolarization ratio.[21] Inserting the depolarization ratio $\varrho = 0.031 \pm 0.008$ based on gas-phase measurements of CH_3CD_3[22] and CD_3I[23] into eq 5, we find that R_{CD_3} is either 0.52 ± 0.05 or 2.3 ± 0.3. For the CN group, a value of $\varrho = 0.04 \pm 0.005$ was reported for acetonitrile in dilute carbon tetrachloride,[24] which leads to R_{CN} equal to 0.48 ± 0.02 or 2.7 ± 0.25. From the Raman data it is not possible to know which of the two choices is correct.

However, using SFG we can tell which value of R is the correct one from measurements of the relative sign of $\chi^{(2)}_{xxz}$ and $\chi^{(2)}_{xzx}$ and its relation to the value of R given in eqs 2 and 3. Using these equations one finds that if the ratio $\chi^{(2)}_{xxz}/\chi^{(2)}_{xzx}$ is positive then R is less than one, whereas if the ratio $\chi^{(2)}_{xxz}/\chi^{(2)}_{xzx}$ is negative then R is greater than one. To our knowledge this capability of SFG to determine R, the ratio of the Raman polarizability elements, has not been previously recognized. To determine the relative sign of the nonlinear susceptibility elements, we measured the magnitude of I_x, which is the intensity of the s-polarized SFG signal, when the infrared and visible input beams were both polarized at 45° from the surface normal and parallel to each other, i.e., both at $\phi = 0°$ or both at $\phi = \pi$, where ϕ is the azimuthal angle in spherical polar coordinates. The value of I_x was then measured with both beams again at 45° to the surface normal but orthogonal to each other, i.e., one at $\phi = 0°$ and the other at $\phi = \pi$. If the signal is larger for the parallel combination, then $\chi^{(2)}_{xxz}$ and $\chi^{(2)}_{xzx}$ are of the same sign; otherwise they are of opposite sign. We see this directly from the expression for the macroscopic s polarization of the sum frequency,

$$P^{\text{sum}}_x = \chi^{(2)}_{xxz} E^{\text{vis}}_x E^{\text{ir}}_z + \chi^{(2)}_{xzx} E^{\text{vis}}_z E^{\text{ir}}_x \quad (6)$$

where E is the incoming electric field amplitude along the laboratory axis indicated by the subscripts. The plane of incidence is the yz plane. If positive z is assumed to be pointing upward along the surface normal, an electric field polarized 45° to the normal will always have a positive projection on the z axis. However, the sign of E_x depends upon which side of the normal the polarization axis is directed, i.e., at $\phi = 0°$ verses $\phi = \pi$. When both the infrared and visible light are polarized parallel to each other the sign of the product of the electric fields in both terms is the same, but when the polarizations of the input beams are orthogonal the sign of the product of the electric fields in the first term is different from that of the second term. Thus the relative sign of the macroscopic susceptibility elements can be determined by comparing the size of the signal for the two polarization combinations. An alternative but experimentally more demanding way to determine the relative sign of the susceptibility elements is to carry out absolute phase measurements.[25,26]

Using the polarization method, we find for the CN vibration the SFG signal is larger for the parallel polarized combination. For the CD_3 vibration the orthogonally polarized combination yields a larger SFG signal. These results indicate that for CN $\chi^{(2)}_{xxz}$ and $\chi^{(2)}_{xzx}$ have the same sign, but for CD_3 $\chi^{(2)}_{xxz}$ and $\chi^{(2)}_{xzx}$ have different signs. From eqs 2 and 3 we see this implies that for CN $R < 1$ and for CD_3 $R > 1$. In the case of the nitrile this is consistent with the expectation that the change in polarizability would be greater parallel to the bond than perpendicular to it and makes 0.48 the favored choice. That $R > 1$ for the CD_3 is consistent with the choices made for R by other workers based on a simple bond polarizability model[20] or based on Raman depolarization measurements.[22,23] In sum frequency experiments[27] the bond polarizability model of the methyl transition was used. It yields an $R_{CD_3} = 4.0$, which differs from the value of 2.3 obtained from Raman measurement of CD_3 vibrations in gas-phase molecules. In the simple bond polarizability model the approximation is made that there is only polarizability parallel to the bond axis, not perpendicular to it. Using a modified and physically more reasonable bond polarizability model[28] that includes both parallel and perpendicular components, we find that a value of R in better agreement with the Raman result is obtained. In our analysis, we use the value of $R = 2.3$ for the CD_3 group. Inserting the measured ratios $\chi^{(2)}_{xxz}/\chi^{(2)}_{xzx}$ for each of the surface densities studied and $R = 2.3$

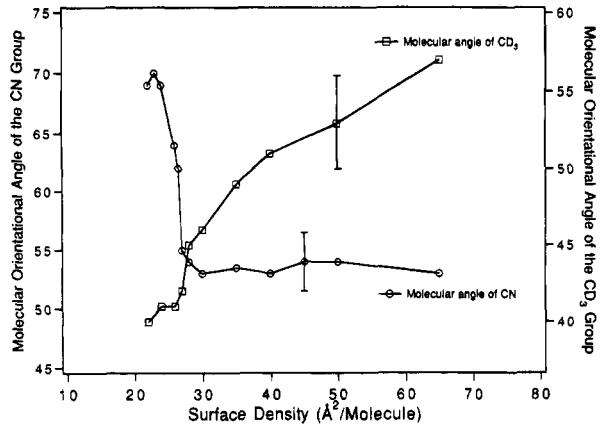

Figure 6. Molecular orientational angle θ with respect to the surface normal for CN head group (in circles) and CD_3 tail (in squares) versus amphiphile surface density.

into eq 4 we obtain the molecular angle for the CD_3 group as a function of surface density, shown in Figure 6. For the CN head group, the ratio $\chi^{(2)}_{xxz}/\chi^{(2)}_{xzx}$ was measured to be 2.1 ± 0.05 the coexistence region and 1.8 ± 0.05 in the condensed-phase region at 24 Å²/molecule. These values are smaller than can be obtained from eq 4 when the value of $R_{CN} = 0.48$ deduced from Raman measurements is used. This suggests that R_{CN} is different in the environment of the monolayer than for the molecule in a nonpolar solvent. Considering the spectral evidence that the CN is interacting strongly with the water subphase, it is not surprising that the ratio of the molecular hyperpolarizabilities of the monolayer is different than that of the molecule in a nonpolar solvent. To obtain the molecular orientation of the CN head group we have combined two different methods. One involves measurement of nonlinear susceptibility elements and yields the molecular angle using eq 4. The second method is based on the relationship between the molecular angle and the measured polarization of the SF light.[29] By imposing the requirement that both methods should yield the same molecular angle for the same molecular polarizability ratio, we found that R equals 0.26. This value of R represents an average covering the coexistence density of 27 Å² to the liquid-phase density of 24 Å². With the value of R = 0.26, agreement between the two methods was obtained for all the surface densities measured. As shown in Figure 6, the orientation of the CN head group remains constant at an angle 53° ± 3° from the surface normal throughout the gas−liquid coexistence region. At the phase transition point, 27 Å², the density is equal to the density of the liquid islands in the coexistence region and consequently has the same molecular angle as shown in Figure 6. Upon further compression, however, the density increases and the molecular angle changes from 53° to 70°, which is closer to the surface plane. For the methyl group, at a density of 65 Å²/molecule in the coexistence region, the molecular angle is found to be 57° ± 4°. Upon compression the molecular orientation of the methyl group continuously shifts from 57° at 65 Å²/molecule to an angle of 42° at the phase transition density of 27 Å²/molecule and then changes only slightly to 40° at 24 Å²/molecule, which corresponds to a 5° tilt for an all-trans chain (Figure 6).

As noted above, the constant orientation for the CN head group throughout the coexistence region measured can be understood by the fact that the intermolecular distance between the head groups of these condensed liquid islands in the gas−liquid coexistence region is the same up to a density of 27 Å²/molecule at which a full monolayer is formed. The compressing process in the coexistence region merely increases the size and number of these liquid islands but does not change the intermolecular spacing and thus does not change the orientation of the head groups. This is also consistent with the result that the chemical environment around head groups did not change throughout the coexistence region, illustrated by the constant value of the CN vibrational frequency shown earlier. When the monolayer is further compressed into the liquid-phase region, the intermolecular distance decreases, which is accompanied by a change in the chemical environment and a consequent change in the orientation of the head group. We believe that this reorientation of the head group is related to the change in balance of intermolecular interactions among the amphiphilic molecules within the monolayer and the hydrophilic head groups of these molecules with the water subphase. As we compress the monolayer into the liquid-phase region, the water molecules between the head groups are squeezed out of the monolayer. With the disappearance of the screening effect from the water molecules and the decrease in the intermolecular distance, the dipole−dipole repulsive interactions, $\mu_{CN} \approx 3.5$ D,[30] are greatly increased. In order to reduce these repulsions, the CN head groups rotate to an orientation closer to the surface plane, approaching the lower energy head to tail configuration. This change in head-group orientation forces a change in the chain orientation and consequently chain−chain interactions. It is this subtle interplay of forces that triggers the phase transition. We thus see that although chain−chain interactions are generally viewed as the dominant factor in the phase transition, with the head groups being assigned a secondary role, the observations presented in these studies suggest that the head-group interactions can be the dominant factor in the phase transition.

Unlike the head group, the observed orientation of the tail (CD_3) of the long-chain molecules is very sensitive to the surface density throughout the gas−liquid coexistence region into the liquid-phase region. This dependence of the orientation on density is believed to be a result of the change in the relative number of amphiphiles close to the perimeters of the islands versus their interior regions. The Gibbs free energy of the system is lowered when the perimeter molecules are allowed to flop over into configurations with the hydrocarbon tails extended in a more horizontal orientation above the water subphase. The molecules in the center of the island exhibit a more upright orientation due to chain−chain interactions. Our data show that the orientation becomes more upright as the monolayer density increases, which is consistent with the fact that the relative number of molecules in the center of the island increases as the island size grows. The continuous change in the average orientational distribution of the tail (CD_3), even in the gas−liquid coexistence region, is markedly different from that of the head group (CN), which does not reorient in the coexistence region. These observations reflect the flexibility of the tails, which extend into the air with more orientational freedom than the strongly solvated and hydrogen-bonded head groups immersed in the water subphase.

Conclusion

We have shown that IR + visible sum frequency generation studies of both the head and tail groups of a long-chain amphiphile reveal important features of the structure and interactions of the head groups, hydrocarbon chains, and aqueous subphase that constitute a Langmuir monolayer interface. Indeed we observe for $CD_3(CH_2)_{19}CN$ at the air/water interface that the orientational dependencies on amphiphile density differ markedly for the CN head group and the CD_3 tail. This has important implications for the monolayer phase behavior.

Throughout the gas−liquid coexistence region, the nitrile head groups are hydrogen bonded with and solvated by water

molecules, as manifested by the blue shift in the CN vibrational frequency. When the amphiphile density exceeds 27 Å^2/molecule, which corresponds to the density at which the phase transition connecting the gas−liquid coexistence and liquid-phase regions occurs, the hydrogen bonds of the head group to water are observed to break. This result suggests that a key step in the phase transition involves rupturing the hydrogen bonds with water and squeezing the water molecules between the CN head groups out of the liquid-phase monolayer. These changes in the chemical environments are correlated not only with spectral shifts but with a structural change in the head-group orientation as well. It was found that the CN head groups rotate from an angle of 53° ± 3°, which is the orientation throughout the gas−liquid coexistence region that we studied (100−27 Å^2), to a more horizontal orientation of 70° ± 3° upon undergoing a phase transition into the liquid-phase region. The sqeezing out of the water molecules leading to a closer approach of the head groups would increase the effect of the dipole−dipole repulsion between the CN groups on the monolayer free energy. By rotation of the head groups to a more horizontal orientation the dipole−dipole repulsions are reduced. These observations raise the possibility that it is the rupturing of the hydrogen bonds of the head groups with water and the reorientation of the head groups that may be the trigger for the phase transition between the gas−liquid coexistence region and the liquid-phase region for this amphiphile.

Unlike the head group, the orientation of the tail is quite sensitive to the monolayer density even in the gas−liquid coexistence region. Our data show that the tail continuously becomes more upright upon compression. We have also observed a frequency shift and a change in the spectral width of the overtone band as the surface density is increased. These results indicate that the CD_3 tail experiences a larger range of local environments at low density in the gas−liquid coexistence region than at the high density of the liquid-phase region. At low density the perimeter amphiphiles of the islands, which are present in the coexistence region, can flop over and thus experience more structural arrangements than at the high density of the liquid-phase region where chain−chain interactions restrict the CD_3 tails to a more upright position.

In addition to what was learned about the behavior of the long-chain amphiphile, we also demonstrated a method for using SFG to remove the ambiguity in the ratio of the Raman polarizability elements ($\alpha_{xx}^{Raman}/\alpha_{zz}^{Raman} > 1$ or $\alpha_{xx}^{Raman}/\alpha_{zz}^{Raman} < 1$) for a totally symmetric transition. Linear Raman depolarization measurements cannot determine whether the ratio is greater than or less than one, whereas SFG can. We find that this ratio is >1 for the CD_3 symmetric stretch and <1 for the CN stretch. This method also yields the relative sign of the two macroscopic susceptibility elements $\chi_{xxz}^{(2)}$ and $\chi_{xzx}^{(2)}$ without the necessity of an absolute phase measurement.

Acknowledgment. We thank Xiaolin Zhao for his advice and help with the monolayer preparation and surface tension measurements and Ruo Xu and William Jenks who provided advice on the synthesis of $CD_3(CH_2)_{19}CN$ and assistance with the NMR. We also thank Professor Nick Turro for the use of his gas chromatography equipment. The authors also thank the Division of Chemical Science of the Department of Energy for their support and the National Science Foundation for their equipment support.

References and Notes

(1) Dutta, P.; Peng, J. B.; Ketterson, J. B.; Parakash, M. *Phys. Rev. Lett.* **1987**, *58*, 2228.
(2) Vaknin, D.; Kjaer, K.; Als-Nielsen, J.; Lösche, M. *Biophys. J.* **1991**, *59*, 1325.
(3) Tung, Y. S.; Fina, L. J.; Gao, T.; Rosen, M. J.; Valentini, J. E. *Proc. A.C.S. Div. Polym. Mater.* **1991**, *65*, 308.
(4) Losche, M.; Sackmann, E.; Mohwald, H. Ber. Bunsenges. *Phys. Chem.* **1983**, *87*, 848.
(5) Weis, R. M.; McMconnell, H. M. *Nature* **1984**, *310*, 3848.
(6) Vogel, V.; Mullin, C. S.; Shen, Y. R.; Kim, M. W. *J. Chem. Phys.* **1991**, *95*, 4620.
(7) Eisenthal, K. B. *Annu. Rev. Phys. Chem.* **1992**, *43*, 627.
(8) Shen, Y. R. *Nature* **1989**, *337*, 519.
(9) Gaines Jr., G. L. *Insoluble Monolayers at Liquid−Gas Interfaces*; Interscience Publishers: New York, 1966.
(10) Moller, M. A.; Tildesley, D. J.; Kim, K. S.; Quirke, N. *J. Chem. Phys.* **1990**, *94*, 8390.
(11) Guyot-Sionnest, P.; Hunt, J. H.; Shen, Y. R. *Phys. Rev. Lett.* **1987**, *59*, 1597.
(12) Hunt, J. H.; Guyot-Sionnest, P.; Shen, Y. R. *Chem. Phys. Lett.* **1987**, *133*, 189.
(13) Copeland, L. E.; Harkins, W. D. *J. Am. Chem. Soc.* **1942**, *64*, 1600.
(14) Zhao, X.; Goh, M. C.; Subrahmanyan, S.; Eisenthal, K. B. *J. Phys. Chem.* **1990**, *94*, 3370.
(15) Zhang, D.; Gutow, J. H.; Eisenthal, K. B.; Heinz, T. F. *J. Chem. Phys.* **1993**, *98*, 5099.
(16) Duncan, J. L.; Kelly, R. A.; Nivellini, G. D.; Tullini, F. *J. Mol. Spectrosc.* **1983**, *98*, 87.
(17) Gayles Jr., J. N.; King, W. T. *Spectrosc. Acta* **1965**, *21*, 543.
(18) Henry, B. R.; Miller, R. J. D. *Chem. Phys. Lett.* **1978**, *60*, 81.
(19) Greenlay, W. R. A.; Henry, B. R. *Chem. Phys. Lett.* **1978**, *53*, 325.
(20) Superfine, R.; Huang, J. Y.; Shen, Y. R. *Chem. Phys. Lett.* **1990**, *172*, 303.
(21) Long, D. A. *Raman Spectroscopy*; McGraw-Hill International Book Company: New York, 1986.
(22) Martin, J.; Montero, S. *J. Chem. Phys.* **1984**, *80*, 4610.
(23) Santos, J.; Orza, J. M. *J. Mol. Struct.* **1986**, *142*, 202.
(24) Whittenburg, S. L.; Wang, C. H. *J. Chem. Phys.* **1977**, *66*, 4255.
(25) Kemnitz, K.; Bhattacharyya, K.; Hicks, J. M.; Pinto, G. R.; Eisenthal, K. B.; Heinz, T. F. *Chem. Phys. Lett.* **1986**, *131*, 285.
(26) Superfine, R.; Huang, J. Y.; Shen, Y. R. *Opt. Lett.* **1990**, *15*, 1276.
(27) Hirose, C.; Akamatsu, N.; Domen, K. *J. Chem. Phys.* **1992**, *96*, 997.
(28) Hirose, C.; Yamamoto, H.; Akamatsu, N.; Domen, K. *J. Phys. Chem.* **1993**, *97*, 10064.
(29) Heinz, T. F. In *Nonlinear Surface Electromagnetic Phenomena*; Ponath, H.-E., Stegeman, G. I., Eds.; Elsevier Science Publishers: New York, 1991; p 353.
(30) Grundnes, J.; Klaboe, P. In *The Chemistry of the Cyano Group*; Rappoport, Z., Eds.; Interscience Publishers: New York, 1970.

JP942518T